Pion inelastic scattering to the three lowest 2^+ states of ^{18}O

S. J. Seestrom-Morris,* D. Dehnhard, M. A. Franey, D. B. Holtkamp,* and C. L. Blilie†
University of Minnesota, Minneapolis, Minnesota 55455

C. L. Morris
Los Alamos National Laboratory, Los Alamos, New Mexico 87545

J. D. Zumbro and H. T. Fortune
University of Pennsylvania, Philadelphia, Pennsylvania 19104
(Received 8 June 1987)

Angular distributions were measured for excitation of the $2_1^+(1.98)$, $2_2^+(3.92)$, and $2_3^+(5.26)$ states of ^{18}O by π^+ and π^- scattering at $T_\pi = 164$ MeV. The data have been compared with distorted-wave impulse-approximation calculations using transition densities from the collective model, from electron scattering, and from the coexistence model. The calculations using (e,e') transition densities reproduce the shapes of the angular distributions very well and the magnitudes of the cross sections to within 15%. The collective-model transition densities fail to fit the data unless the radius is adjusted from the ground-state value.

I. INTRODUCTION

Comparisons of π^+ and π^- inelastic scattering in the region of the [3,3] resonance have proven useful for extracting neutron and proton transition strengths. For example, very large differences between π^+ and π^- inelastic cross sections have been observed for $M4$ (unnatural-parity) transitions to "stretched" states in p-shell nuclei. These data[1-3] showed that some transitions are dominated by either pure proton or neutron particle-hole excitations. For this class of transitions the π^+/π^- cross-section ratios are well understood in terms of $1\hbar\omega$ shell-model calculations and distorted-wave impulse-approximation (DWIA) calculations. In addition, the strengths extracted are generally in good agreement with those determined from the scattering of other hadronic and electromagnetic probes. These transitions are well suited to probing by pion inelastic scattering since they involve the same orbitals for neutrons and protons and the transition densities are peaked near the nuclear surface where pion scattering should be most sensitive.

The nucleus ^{18}O is one for which large differences are expected between π^+ and π^- scattering to low-lying, natural-parity states. The simple shell-model description of this nucleus assumes two neutrons in the $(2s1d)$ shell coupled to a closed-shell ^{16}O core. Thus, low-lying 2^+ states, formed by rearranging the two valence neutrons, can be reached only by pure *neutron* transitions from the ground state. The coexistence model[4] combines the two-particle–zero-hole (2p-0h) states of the simple shell model with deformed collective states.

Pion inelastic scattering on ^{18}O has been studied previously by Iversen *et al.*[5] and Lunke *et al.*[6] At $T_\pi = 164$ MeV the ratio $R = \sigma(\pi^-)/\sigma(\pi^+)$ for the 2_1^+ state was determined[5] to be 1.86 ± 0.16 and at $T_\pi = 180$ MeV it was found to be 1.58 ± 0.15, at both energies much smaller than the value of $R \simeq 9$ expected for a pure neutron transition. This supported the well-known fact[4,7] that the simple shell model is insufficient to describe the low-lying levels of ^{18}O. Oset and Strottman[8] compared the early data for the 2_1^+ state[5] to Glauber-model calculations and concluded that core-polarization effects are needed to describe the π^-/π^+ cross-section ratio.

Lee and Lawson[9] discussed the pion data[5] in the context of momentum-space DWIA calculations using three different models for the ^{18}O wave functions. They concluded that the data for the 2_1^+ state and an unresolved peak near 3.9 MeV, which is dominated by the 2_2^+ state, could be described by models that also reproduce the electromagnetic data. The third 2^+ state (5.26 MeV) was not resolved from the strongly-excited 3^- state at 5.10 MeV. Thus it was not possible to verify the large enhancement of the 2_3^+ state in π^+ scattering predicted by the model of Ref. 4.

In this paper we present angular distributions of π^+ and π^- scattering at $T_\pi = 164$ MeV for the transitions to the 2_1^+ (1.98 MeV), 2_2^+ (3.92 MeV), and 2_3^+ (5.26 MeV) states of ^{18}O. The energy resolution was improved over that attained in the earlier experiments[5,6] and the background was less severe. Although the 2_3^+ and 3_1^- states were not completely resolved, we successfully extracted cross sections for both by peak fitting. These data are compared with DWIA calculations using transition densities from different models. The cross sections extracted for the 2_2^+ and 2_3^+ states allow a more detailed test of the various models than was possible using the data of Ref. 5.

II. EXPERIMENT

The energetic pion channel and spectrometer (EPICS) at the Clinton P. Anderson Meson Physics Facility was used to make the measurements. The EPICS system has

been described in detail elsewhere.[10] Data were obtained for π^+ and π^- scattering at an incident pion kinetic energy $T_\pi = 164$ MeV for laboratory scattering angles between 18° and 74°. The energy resolution was about 240 keV (FWHM).

The target was oxygen gas isotopically enriched to 94.9% in ^{18}O (3.4% ^{16}O and 1.7% ^{17}O) contained in a cylinder of 12.7 cm diameter and 23 cm height. The cylinder walls were nickel foils of thickness 0.025 mm. The horizontal and vertical extent of the target was larger than the size of the EPICS beam spot. The target gas was cooled to a temperature of 118 K and kept at a pressure of 1.8 atm. The target temperature and pressure were monitored as a function of time. The target density, as measured by the ratio of pressure of temperature (P/T), was found to be constant to better than 1.4%. An average areal target density of 76 mg/cm^2 for ^{18}O was calculated from the average value of P/T and the geometry, and used in the analysis of all the ^{18}O data runs.

Because of the large extent of the target in the direction (z) of the incident pion momentum, the target volume viewed by the spectrometer is a function of the scattering angle. Pions scattered at small angles ($\leq 25°$) from any z position in the target are included in the spectrometer acceptance. At larger angles, however, pions scattered at the edges of the target will not be included. Therefore, yields for $\pi^+ - p$ scattering were measured at each angle in order to determine the absolute cross section normalizations by comparing the yields with $\pi^+ - p$ cross sections (calculated from the phase shifts of Ref. 11). The relative π^+/π^- normalization was obtained from the comparison of $\pi^- - p$ yields at two angles with predicted $\pi^- - p$ cross sections. Both the π^+ and π^- yields from hydrogen were measured using methane as a target gas.

Yields for the inelastic transitions were extracted with a peak-fitting code[12] that used the experimental line shape to fit normalized spectra of $d^2\sigma/d\Omega\, dE$ vs excitation energy. The excitation energy region from 1 MeV to 6 MeV was fitted including the following states; 2_1^+ (1.98 MeV), 4_1^+ (3.56 MeV), 2_2^+ (3.92 MeV), 1_1^- (4.45 MeV), 3_1^- (5.10 MeV), and 2_3^+ (5.26 MeV). The separation of each state from the 2_1^+ state was fixed at the difference in excitation energies.[13] Contributions from the 0_3^+ (5.33 MeV) and 3^+ (5.37 MeV) states were assumed to be negligible. The angular distributions extracted for the 4^+ state indicate some contribution at forward angles due to the unresolved 0_2^+ (3.63 MeV) state. The peak near 5.1 MeV is expected to be dominated by the 3^- state (5.10 MeV). In the π^+ spectra the peak was broader than the 2_1^+ peak at angles forward of 38° and could not be fitted satisfactorily without the inclusion of the 5.26-MeV 2_3^+ state. Figure 1 shows spectra and fits for π^+ and π^- scattering at 30°. Only the data for the three 2^+ states are presented in this work; the data for the 1_1^- and 3_1^- states have been presented in a previous publication.[14]

Corrections were applied to the data to account for computer live time, chamber efficiency, pion survival fraction, and momentum dependence of the spectrometer acceptance. The uncertainties in these corrections lead to a systematic uncertainty in the cross sections of 4.5%. The uncertainty in the absolute normalization is 6%, which includes the uncertainty in the ^{18}O and CH_4 target thicknesses, the uncertainty in the calculated $\pi - p$ cross sections due to the uncertainties in the incident pion energy, scattering angle, and $\pi - p$ phase shifts, and the statistical uncertainty in the $\pi - p$ yields. These factors result in an overall uncertainty in the data of 8%. The error bars plotted with the data points include only the statistical and peak-fitting errors.

III. RESULTS AND ANALYSIS

A. Discussion of the data

The angular distributions for the 2^+ states at 1.98, 3.92, and 5.26 MeV in ^{18}O measured at $T_\pi = 164$ MeV, are plotted in Figs. 2–4. The 2_1^+ state is enhanced in π^- scattering compared to π^+ by a factor $R = 2.10 \pm 0.16$ at

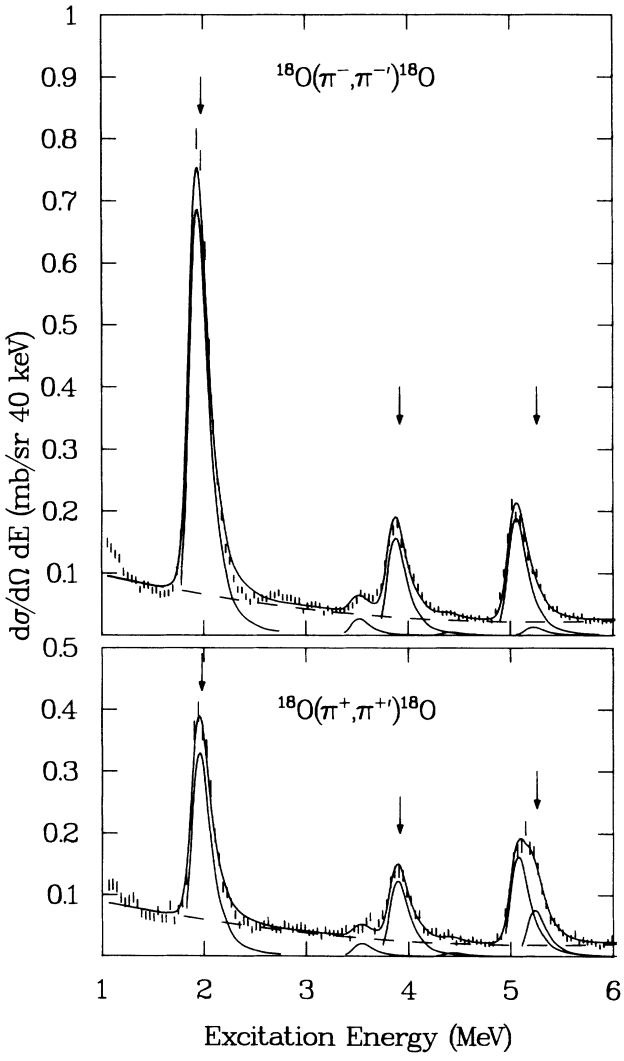

FIG. 1. Typical spectra and fits with the program FIT for ^{18}O(π^+,$\pi^{+\prime}$) and ^{18}O(π^-,$\pi^{-\prime}$) at $\theta_{lab} = 30°$.

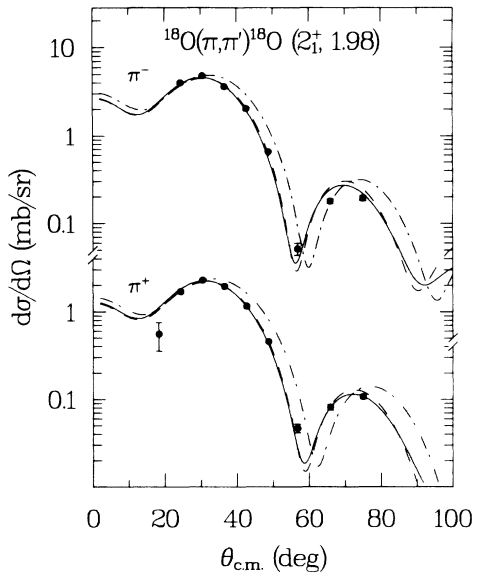

FIG. 2. Angular distributions for the 2_1^+ state at 1.98 MeV in ^{18}O measured at $T_\pi = 164$ MeV. The calculated curves were generated using transition densities from the collective model (dot-dashed lines), the modified collective model (dashed lines), and the Fourier-Bessel expansion (solid lines).

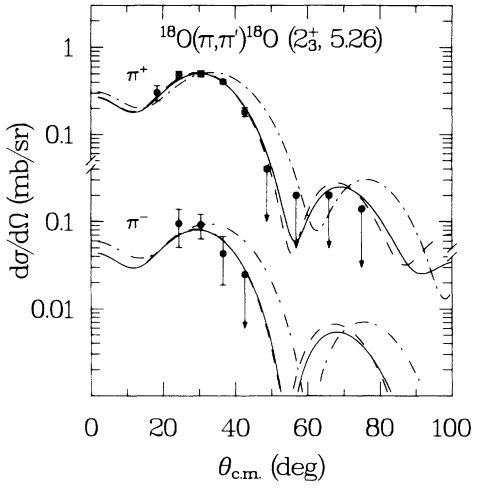

FIG. 4. Angular distributions for the 2_3^+ state at 5.26 MeV in ^{18}O at $T_\pi = 164$ MeV. The theoretical curves were generated as in Fig. 2.

30°. This ratio is slightly larger than the value quoted in Ref. 5, $R = 1.86 \pm 0.16$, and significantly larger than the value $R = 1.58 \pm 0.15$ obtained[6] at $T_\pi = 180$ MeV. We found that our elastic π^+ data are 16% lower, our elastic π^- data are 5% lower, and both the π^+ and π^- inelastic cross sections for the 2_1^+ state are 25% lower than those of Ref. 5. Our forward-angle elastic data are in better agreement with DWIA calculations. Also, the shapes of the 2_1^+ angular distributions of Ref. 5 indicate that the peak fitting has substantially overestimated the cross sections at the far forward angles. This is partly due to the difficulty in subtracting the tail of the elastic peak when the resolution is relatively poor.

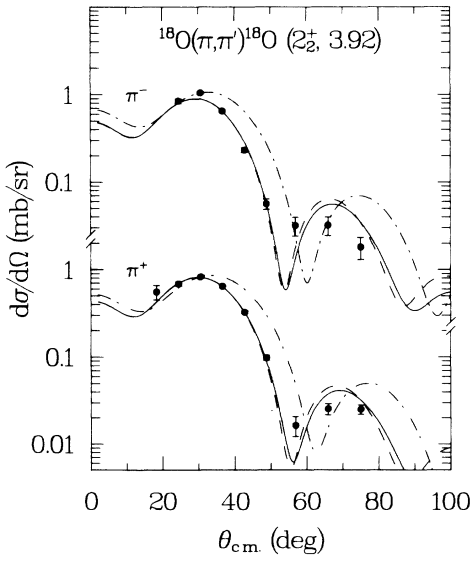

FIG. 3. Angular distributions for the 2_2^+ state at 3.92 MeV in ^{18}O at $T_\pi = 164$ MeV. The theoretical curves were generated as in Fig. 2.

For the 2_2^+ state at 3.92 MeV, the π^-/π^+ cross section ratio is $R = 1.3 \pm 0.1$. The minima in both π^+ and π^- angular distributions occur at a slightly smaller angle than for the first 2^+ state. In the previous (π,π') study[5] of ^{18}O this state was not resolved from the neighboring 4^+ (3.56 MeV) and 0^+ (3.63 MeV) states. We find that at 30° the $(4^+,0^+)$ doublet has about 20% of the 2_2^+ yield whereas near 56° the yield for the $(4^+,0^+)$ doublet is two to three times larger than for the 2_2^+ state.

In contrast to the first two 2^+ states, the third 2^+ state (5.26 MeV) is excited much more strongly by π^+ scattering than by π^-. The ratio at 30° is $R = 0.18 \pm 0.06$ $(1/R = 5.5 \pm 1.8)$. Because of the proximity of the strong 3^- state (5.10 MeV), it was possible to extract π^- cross sections only near the maximum in the 2^+ angular distribution (24° to 36°).

B. DIWA analysis

DWIA calculations were performed using the coordinate-space code DWPI.[15] This code was modified to calculate transition densities from a Fourier-Bessel expansion. The code was also reorganized in order to link it to an optimizer[16] to allow us to search on the parameters of the transition densities. The spin-dependent parts of the pion-nucleon interaction are not calculated in DWPI, but these are not important for the lowest three 2^+ states since they are known to have very small transverse form factors.[17]

The elastic scattering cross sections and the distortions for the inelastic scattering were calculated using a three-parameter Fermi function for the ^{18}O ground-state density. The parameters of this distribution were $c = 2.608$ fm, $z = 0.458$ fm, and $w = -0.051$ for both neutrons and pro-

tons. These parameters were obtained from the ^{16}O charge distribution[17] by decreasing the diffusivity so that the mean-square radius of the point-proton distribution was equal to the mean-square charge radius minus (0.8 fm)^2 to account approximately for the finite size of the proton. Following the prescription of Ref. 18, the π-nucleon phase shifts were evaluated at an energy 28 MeV below the pion-nucleon center-of-mass energy. These parameters gave a good description of the elastic scattering data.

Several models were used to calculate the transition densities for the 2^+ states. The first was a collective model which used

$$\rho^{\rm tr}_{\rm n,p}(r)=\beta_{\rm n,p}c\frac{d\rho_{\rm n,p}(r)}{dr} \ . \tag{1}$$

Here $\rho_{\rm n,p}$ are the ground state densities, $\rho^{\rm tr}_{\rm n,p}$ are the corresponding transition densities and $\beta_{\rm n,p}c$ are the deformation lengths for neutrons and protons. In the second, the "modified" collective model, the transition density was calculated from the derivative of a density with a shape different from that of the ground state. A third model used the Fourier-Bessel expansion with coefficients determined from electron scattering plus additional scaling factors for neutrons and protons. In a fourth prescription, we calculated transition densities from the wave functions of Lawson, Serduke, and Fortune[4] (LSF).

C. Comparison with the data

1. Collective model

The dot-dashed curves plotted in Figs. 2–4 result from DWIA calculations using a collective-model transition density with the neutron and proton deformation parameters $\beta_{\rm n}$ and $\beta_{\rm p}$ adjusted to give the best fit to the π^+ and π^- data at 30°. The experimental angular distributions for the 2^+_1 state are shifted systematically for both π^+ and π^- by about 2° toward smaller angles in comparison with the collective-model calculation (Fig. 2).

The collective-model calculation gives an even less satisfactory description of the angular distribution shapes for the 2^+_2 state (Fig. 3). In this case the shift is about 5°. There is evidence for the same effect in the data for the 2^+_3 state (Fig. 4).

Since these calculations provide an inadequate description of the angular distribution shapes for all three states, values of $\beta_{\rm n}$ and $\beta_{\rm p}$ were determined by normalizing to only the 30° data points where the angular distributions peak. Then neutron and proton matrix elements, $M_{\rm n}$ and $M_{\rm p}$, were calculated from the expression,

$$M_{\rm n,p}=\int r^4\rho^{\rm tr}_{\rm n,p}(r)dr \ . \tag{2}$$

The results are listed in the first row of Table I.

An attempt was made to improve the fits by varying the radius parameter of the distribution whose derivative was used to calculate the transition density (modified collective model). This was done in addition to varying $\beta_{\rm n}$ and $\beta_{\rm p}$ to obtain the best fit to all of the π^+ and π^- data points. The resulting fits are plotted as dashed curves in Figs. 2–4. The best-fit transition densities were obtained by increasing the radius parameter c (for both neutrons and protons) from 2.608 to 3.085 fm for the 2^+_1 state and to 3.609 fm for the 2^+_2 and 2^+_3 states. For these values of c the root-mean-square radii of the transition densities, defined by $\{\langle\rho_{\rm tr}r^4dr\rangle/\langle\rho_{\rm tr}r^2dr\rangle\}^{1/2}$, are 3.56 fm and 4.03 fm, compared to 3.16 fm for the unmodified collective model. The values of $M_{\rm n}$ and $M_{\rm p}$ obtained from this set of calculations are listed in the second row of Table I.

2. Fourier-Bessel transition densities

A third set of calculations was performed using transition densities determined in a recent analysis of electron scattering[17] from ^{18}O by fitting coefficients of a Fourier-Bessel expansion to the measured (e,e′) form factors. The finite charge distribution of the proton was not unfolded in the calculations presented here. We tested the effect of unfolding the proton charge distribution and found that

TABLE I. Comparison of matrix elements determined from (π,π') analysis with those from other experiments and theory.

Analysis	$M_{\rm p}$	$M_{\rm n}^{2^+_1}$	$M_{\rm n}/M_{\rm p}$	$M_{\rm p}$	$M_{\rm n}^{2^+_2}$	$M_{\rm n}/M_{\rm p}$	$M_{\rm p}$	$M_{\rm n}^{2^+_3}$	$M_{\rm n}/M_{\rm p}$
(π,π')[a]	5.8(5)	14.1(8)	2.43(27)	4.48(35)	6.0(4)	1.34(14)	5.2(4)	$\leq$0.7	$\leq$0.2
(π,π')[b]	5.4(5)	12.4(7)	2.32(24)	4.41(30)	4.69(31)	1.06(10)	5.0(3)	$\leq$0.2	$\leq$0.1
(π,π')[c]	5.8(5)	13.2(7)	2.29(23)	4.51(31)	4.88(32)	1.08(10)	5.1(3)	$\leq$0.3	$\leq$0.1
(e,e′)[d]	6.69(10)			4.71(10)			5.32(14)		
Lifetime	6.41(10)[e]	16.1(7)[f]	2.51(13)		3.1(8)[g]	0.66(17)[h]			
Hadron[i]			2.5(9)			0.56(31)			
LSF			2.04			1.04			0.25

[a]This work, collective model.
[b]This work, "modified" collective model.
[c]This work, Fourier-Bessel transition density.
[d]Reference 13.
[e]Reference 15.
[f]Reference 17.
[g]Reference 11.
[h]Calculated from the (e,e′) $M_{\rm p}$ and the lifetime $M_{\rm n}$.
[i]Reference 18.

it caused a small shift in the angle of the minimum in the angular distribution. We have not included these calculations because the unfolding procedure generated extra "bumps" in the transition density that seemed unphysical.

We first assumed the neutron transition densities to have the same shape as the proton transition densities. In order to better fit the π^+ and π^- data we introduced scaling factors for both neutrons and protons. The theoretical curves, with the scaling factors adjusted to give the best fit to the data, are plotted as the solid curves in Figs. 2–4. The fits to the experimental angular distributions are very good as in the case of the modified collective model. The values of M_n and M_p determined from these fits are listed in Table I, third row. The scaling factors are included in the values of M_n and M_p. For the proton matrix elements, the factors are 0.86, 0.96, and 0.96, for the 2_1^+, 2_2^+, and 2_3^+ states, respectively.

We also calculated the cross sections for all three 2^+ states by fixing the proton transition density to the results from (e,e′) and varying only the normalization of the neutron transition densities. For the first 2^+ state the best-fit cross sections are about 10% below the π^- and 15% above the π^+ data. The reduced χ^2 for this fit was 35 compared with 6 when the proton normalization was also allowed to vary. For the 2_2^+ and 2_3^+ states the reduced χ^2 was not affected much by constraining the proton transition density to the (e,e′) values. The need for scaling the proton transition density from electron scattering for the 2_1^+ state by a factor of 0.86 in order to fit the pion data is not understood; however, the uncertainty quoted in the (e,e) matrix element is very small (1.5%) and even a 6% uncertainty would result in agreement with our value.

3. *LSF wave functions*

We have also attempted to describe our data guided by the LSF wave functions[4] for the low-lying states of ^{18}O. In the LSF model natural-parity states in ^{18}O are formed from a basis consisting of 2 neutrons in the $(2s1d)$ shell (with no more than one in the $1d3/2$ shell) outside a closed ^{16}O core, plus three collective states of spin and parity 0^+, 2^+, and 4^+. Wave functions were determined[4] by fitting the available one- and two-nucleon transfer data, the $M1$ and $E2$ transition rates, and the static moments. Thus, we construct the proton and neutron transition densities, $\rho_{p,i}$ and $\rho_{n,i}$, as

$$\rho_{p,i}(r)=\gamma_i\rho_{\rm coll}(r)+e_n A_{n,i}(r) , \tag{3}$$

and

$$\rho_{n,i}(r)=\gamma_i\rho_{\rm coll}(r)+e_p A_{n,i}(r) , \tag{4}$$

where $\rho_{\rm coll}(r)$ is the (isoscalar) transition density for the collective 2^+ state and $A_{n,i}(r)$ are the contributions from the states of the $(2s1d)^{2n}$ configurations of the LSF model. The subscript $i=1$, 2, or 3 refers to the 2_1^+, 2_2^+, or 2_3^+ states, respectively. The (state-dependent) factors γ_i were taken from LSF. The (state-independent) effective charges, e_n and e_p, were fixed at 0.5 and 1.5, respectively. The neutron single-particle components (A_n) contribute to the proton transition density because the valence neutrons polarize the proton core; similarly, if there were valence protons they would contribute to the neutron transition density by polarizing the neutron core.

Lee and Lawson[9] have pointed out that these wave functions underestimate the $B(E2;0_1^+\rightarrow 2_2^+)$. Furthermore, recent measurements of $B(E2;0_1^+\rightarrow 2_1^+)$ (Ref. 19) and $B(E2;0_1^+\rightarrow 2_3^+)$ (Ref. 13) find larger values for these quantities than the LSF model predicts. We found that if the collective matrix elements of the constrained II fit of Ref. 4 are increased by factors of 1.37,1.45,1.58 for the 2_1^+, 2_2^+, and 2_3^+ states, respectively, then the values of M_p for the 2^+ states determined by Norum *et al.*[17] are reproduced. In these calculations of M_p, contributions from the $(2s1d)^{2n}$ components were included with an effective charge $e_n=0.5$. In LSF, the wave function amplitudes are reasonably well-determined by particle-transfer data; the experimental electromagnetic properties serve primarily to fix the properties of the collective intruder states.

In the DWIA calculations the proton transition density was taken to be the charge transition density of Ref. 17. The finite nucleon size was not unfolded. The neutron densities [Eq. (4)] were obtained in the following way. The radial shape of $\rho_{\rm coll}(r)$ was taken from the collective model [Eq. (1)] with a radius parameter $c=3.085$ fm. The magnitude of $\rho_{\rm coll}(r)$ was chosen so that Eq. (2) yielded 1.58 times the LSF collective matrix element. We note that the factor 1.58 is slightly smaller than the factor $1+\delta_c=1.753$ introduced in Ref. 9 in order to fit the early pion cross sections[5] which are about 25% larger than our values. The radial dependence of $A_{n,i}(r)$ was then obtained for each state by solving Eq. (3) using the charge transition density from (e,e′) for $\rho_{p,i}(r)$ and our renormalized $\rho_{\rm coll}(r)$. The essence of this calculation is that the LSF model is used to relate the shape and magnitude of the neutron transition densities to the known proton transition densities.

The angular distributions calculated using the transition densities described above are plotted in Fig. 5. Overall the data for all three 2^+ states are described well, in particular the different ratios of $\sigma(\pi^-)/\sigma(\pi^+)$ are reproduced for the first and second 2^+ states. The agreement is poor only for π^- scattering to the third 2^+ state for which the predicted cross section is a factor of 2 to 3 larger than the data. The angular distribution predicted for π^- is quite different from that for π^+. Because of the node near the surface in the neutron transition density (see Sec. III C 4), the π^- cross section is very sensitive to the radius used for the collective piece of the transition density and it is therefore not surprising that the predicted π^- cross sections disagree with the measured ones. The ratios M_n/M_p from this calculation for all three states are listed in Table I.

4. *Transition densities*

The fitted proton transition densities for the three 2^+ states are plotted in Fig. 6. The dot-dashed curve is $\rho_p^{\rm tr}(r)$ from the collective model, the solid curve represents the

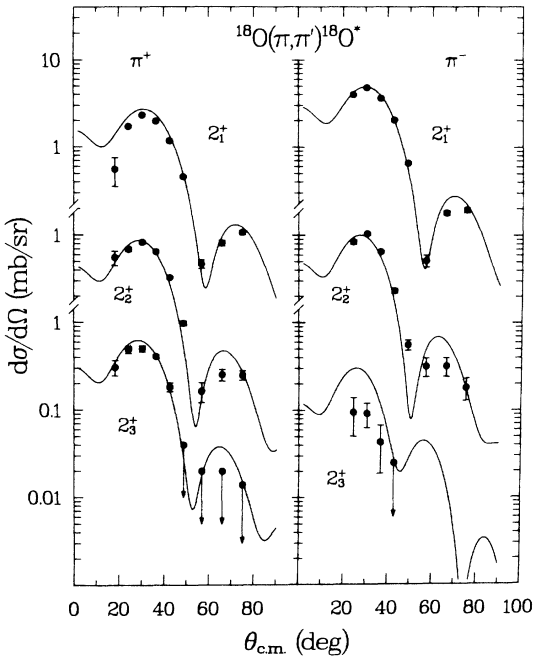

FIG. 5. Angular distributions for the 2_1^+ (top), 2_2^+ (center), and 2_3^+ (bottom) states of ^{18}O for π^+ on the left and π^- on the right. The curves are calculated using the LSF-model transition densities described in the text and presented in Fig. 6.

Fourier-Bessel transition density, and the dashed line is $\rho_p^{tr}(r)$ from the modified collective model. The experimental angular distributions rule out the collective-model transition density because it generates such a poor fit. However, use of the modified collective and Fourier-Bessel transition densities results in very similar angular distributions both being in good agreement with the data. Apparently, the large differences in $\rho^{tr}(r)$ at $r<3.50$ fm (see Fig. 6) do not affect the calculated pion cross sections. Due to strong absorption, (π,π') is most sensitive to ρ^{tr} for $r \geq 3$ fm.

The calculations discussed above (except for LSF) all had identical geometries for the neutron and proton transition densities. We found some evidence that the neutron transition density should have a different shape from that of the protons. The reduced χ^2 for fits to the 2_1^+ data in which the neutron geometry was varied, were about a factor of 2 smaller than when the neutron geometry was kept the same as the proton geometry. The LSF model suggests different shapes for the neutron and proton transition densities as shown in Fig. 7, especially for the 2_2^+ and 2_3^+ states. The neutron densities have nodes near the nuclear surface but the proton densities do not. For the 2_3^+ state these densities generate angular distributions which are very different for π^- and π^+ scattering. Unfortunately, the large error bars on the π^- data preclude testing the shape of the theoretical neutron transition density in this case. We note that the plotted Fourier-Bessel and LSF model proton densities differ by an overall minus sign for the 2_2^+ and 2_3^+ states. The absolute sign cannot be obtained from (e,e') and is irrelevant in a DWIA calculation. However, it would affect coupled channels predictions.

D. Discussion

The neutron and proton matrix elements extracted from our (π,π') data depend on the shape used for the transition densities. If one excludes the collective model,

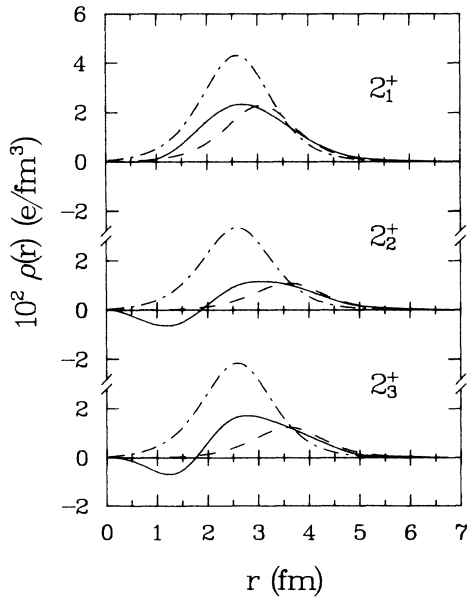

FIG. 6. Proton transition densities for the three 2^+ states; for the collective model (dot-dashed lines), the modified collective model (dashed lines), and the Fourier-Bessel expansion (solid lines).

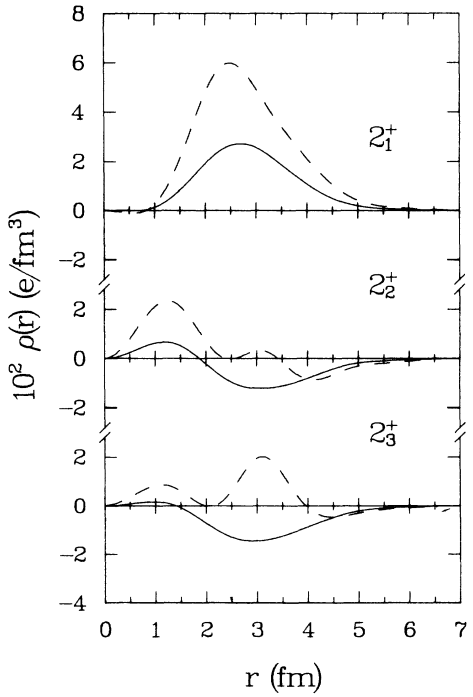

FIG. 7. LSF-model transition densities for protons (solid lines) and neutrons (dashed lines) for the three 2^+ states.

which does not fit the shape of the angular distributions, the variation in matrix elements between the modified collective and Fourier-Bessel transition densities is less than 5%, which is smaller than the experimental uncertainty. When all parameters (c,z,w) of a "modified" collective-model transition density were allowed to vary, the resulting M_p and M_n differed by as much as $\pm 8\%$ about the average value. This variation would be less if the proton densities were constrained to have the shape determined by (e,e').

We have compared our matrix elements with those extracted from other experiments (Table I). As mentioned earlier, the M_p for the 2_2^+ and 2_3^+ state transitions are in good agreement with those from the recent (e,e') analysis. For the 2_1^+ state, however, our M_p is 14% lower than that from (e,e'). The weighted mean[19] of proton matrix elements calculated from the lifetime measured by the recoil distance method, $6.4+0.1$ efm^2, is almost within errors of our average value. An estimate of the neutron matrix elements in ^{18}O can be obtained[9,20] from the proton matrix elements[21] in the mirror nucleus ^{18}Ne (Table I). For the 2_1^+ our M_n is smaller than the mirror-nucleus estimate but the M_n/M_p are in good agreement. The M_n/M_p ratio determined from low-energy nucleon scattering[22] also agrees very well with our result.

For the 2_2^+ state, our neutron matrix element is a factor of 1.6 larger than from the mirror-nucleus measurement, but the latter has a large error bar. The excitation energies of the 2_2^+ states in ^{18}O and ^{18}Ne are different, 3.92 MeV versus 3.62 MeV. Therefore it is possible that the wave functions of the protons in ^{18}Ne are significantly different from those of the neutrons in ^{18}O. To the extent that this is true, the M_p in ^{18}Ne is not a good estimate of the M_n in ^{18}O. The low-energy nucleon scattering[22] experiment yields a value of M_n/M_p for the 2_2^+ state, 0.56 ± 0.31, which is also smaller than our result.

For the 2_3^+ state neither mirror nucleus nor nucleon scattering values exist for M_n/M_p. Our value is an upper limit of ~ 0.1 which is significantly smaller than the LSF value (0.25).

Brown, Bernstein, and Madsen[23] have pointed out a "reversal" effect in a series of nuclei from ^{18}O to ^{90}Zr. Apparently there exists a 2^+ state above the first 2^+ for which the inequality $M_n/M_p > N/Z$ (or $<$) is reversed from the one for the first 2^+ state. For ^{18}O this is based on the mirror-nucleus data for the 2_2^+ state. Although our value of M_n/M_p is larger than the mirror-nucleus value, it still indicates the reversal effect in that it is less than N/Z while for the 2_1^+ state M_n/M_p was greater than N/Z. However, it is likely that the third 2^+ state should be identified with the "reversal" state since M_n/M_p is even smaller than for the second 2^+.

IV. SUMMARY

Our ^{18}O(π,π') data can be described quite well using charge transition densities from (e,e') to give the shape of the transition density for both neutrons and protons. For the 2_1^+ state the value of M_p is slightly smaller than the electromagnetic values. For the 2_2^+ and 2_3^+ states, our values of M_p agree well with those from (e,e').

The coexistence model of Ref. 4 reproduces very well the different values of M_n/M_p for the lowest two 2^+ states using state-independent effective charges. For the third 2^+ level our result is significantly smaller than the LSF value.

The good agreement between the ratio M_n/M_p that we have extracted for the first 2^+ state, and the value from mirror nucleus measurements gives us confidence in the matrix element ratios which we have determined for states in which there are no mirror nucleus data. The ratio M_n/M_p is much less model-dependent than are the individual magnitudes.

This work was supported in part by the U.S. Department of Energy.

*Present address: Los Alamos National Laboratory, Los Alamos, NM 87545.

†Present address: Mission Research Corporation, Santa Barbara, CA 93102.

[1]D. Dehnhard *et al.*, Phys. Rev. Lett. **43**, 1091 (1979).

[2]D. B. Holtkamp *et al.*, Phys. Rev. C **31**, 957 (1985).

[3]S. J. Seestrom-Morris *et al.*, Phys. Rev. C **31**, 923 (1985).

[4]R. D. Lawson, F. J. D. Serduke, and H. T. Fortune, Phys. Rev. C **14**, 1245 (1976).

[5]S. Iversen *et al.*, Phys. Rev. Lett. **40**, 17 (1978); and Phys. Lett. **82B**, 51 (1979).

[6]C. Lunke *et al.*, Phys. Lett. **78B**, 201 (1978).

[7]P. J. Ellis and T. Engeland, Nucl. Phys. **A144**, 161 (1970).

[8]E. Oset and D. Strottman, Phys. Lett. **84B**, 396 (1979).

[9]T.-S. H. Lee and R. D. Lawson, Phys. Rev. C **14**, 679 (1980).

[10]H. A. Thiessen *et al.*, Los Alamos Scientific Laboratory Report LA-4534-MS (unpublished).

[11]G. Rowe, M. Saloman, and R. H. Landau, Phys. Rev. C **18**, 584 (1978).

[12]C. L. Morris, Computer Program FIT (unpublished).

[13]F. Ajzenberg-Selove, Nucl. Phys. **A392**, 1 (1983).

[14]S. Chakravarti *et al.*, Phys Rev. C (to be published).

[15]R. A. Eisenstein and G. A. Miller, Comput. Phys. Commun. **11**, 95 (1976).

[16]F. James and M. Roos, Comput. Phys. Commun. **10**, 343 (1975).

[17]B. E. Norum *et al.*, Phys. Rev. C **25**, 1778 (1982).

[18]W. B. Cottingame and D. B. Holtkamp, Phys. Rev. Lett. **45**, 1828 (1980).

[19]G. C. Ball *et al.*, Nucl. Phys. **A377**, 268 (1982).

[20]A. M. Bernstein, V. R. Brown, V. A. Madsen, Phys. Rev. Lett. **42**, 425 (1979); *ibid.* **103B**, 255 (1981); and Comments Nucl. Part. Phys. **11**, 203 (1983).

[21]A. B. McDonald *et al.*, Nucl. Phys. **A258**, 152 (1976).

[22]P. Grabmyr, J. Rapaport, and R. W. Finlay, Nucl. Phys. **A350**, 167 (1980).

[23]V. R. Brown, A. M. Bernstein, V. A. Madsen, Phys. Lett. **164B**, 217 (1985).